

**TIME RESOLUTION OF DOWNCORE CHEMICAL CHANGES
IN LAKE ERIE SEDIMENTS**

S6, 15-95

Gerald Matisoff
Department of Geological Sciences
Case Western Reserve University
Cleveland, Ohio 44106
Tele: (216)368-3677
Fax: (216) 368-3691
email: gxm4@po.cwru.edu

ABSTRACT

Burrowing and feeding activities of benthic macroinvertebrates mix surficial sediment and cause a loss of time resolution in sediment cores. However, recent stable isotopic analyses of organic matter in sediment cores suggests that events that occur over as little as a season may be identifiable. This work addresses this apparent discrepancy between historical records derived from downcore sediment tracer concentrations with sediments that are biologically mixed.

Simulations of a surface mixed layer of finite thickness which overlies a sediment layer in which there is no mixing are performed to illustrate the nature of the loss of time resolution in Lake Erie sediments caused by mixing. Variations in the sedimentation rate, mixed depth interval, tracer half-life, and biodiffusion coefficient are examined to determine conditions in which annual or interannual changes can be expected to be identifiable in the sediment record. In some areas of Lake Erie where the sedimentation rate is high it is possible to distinguish interannual differences of 3-7 years, but it is still unclear if annual changes can be identified.

INTRODUCTION

Nutrient and contaminant loadings to Lake Erie increased slightly after European settlement in the last half of the 19th century and increased considerably more in the 20th century. These historical changes in pollutant loadings to Lake Erie resulted in well documented changes in primary productivity and bioaccumulation of toxics. Recent management measures for controlling phosphorus and some contaminant loadings may have reversed the eutrophication and some bioaccumulation trends. One method to evaluate natural excursions in water quality and the impact of past anthropogenic effects and management controls on water quality is to examine downcore changes of sediment proxies of lake productivity and water quality.

Usually, an increase in depth is an increase in sediment age. However, reconstruction of the historical record from downcore chemical changes is complicated by post-depositional processes such as diagenesis (Matisoff and Holdren, 1995) and biological mixing (Matisoff, 1984). Paleolimnological reconstructions of the Great Lakes are limited by a loss of time resolution associated with biological mixing. Benthic macroinvertebrates, through their burrowing and feeding activities redistribute sediment particles from several depths and smear the sediment record. This sediment redistribution results in a loss of time resolution by mixing the first appearance of microfossils or chemical tracers down into sediments that are older than those in which the appearance occurred and in the retention of the last appearance of microfossils or chemical tracers in sediments that are younger than those in which the extinction occurred (Berger and Heath, 1968). It is important to note that in mixed sediments the age assigned to any sediment depth is not a unique age for that depth interval. Rather, the sediment in any depth interval is composed of different proportions of sediments of various ages and that the sediment is best

thought of in terms of an age frequency distribution (Davis, 1974).

The biologically mixed sediment column can be described as a surface mixed layer of finite thickness which overlies a sediment layer in which there is no mixing (Goldberg and Koide, 1962). If the surface layer is mixed rapidly relative to the rate of sedimentation, then any deposition onto the sediment surface will be uniformly redistributed throughout the mixed zone and some will be mixed into the top of the undisturbed sediment below. Separate depositional events cannot be resolved for times less than the residence time of sediment within the mixed zone. This residence time is referred to as the time resolution or intrinsic resolution and can be defined as the time between two successive input tracer pulses which results in a profile preserved below the mixed zone in which there are still two identifiable peaks (Robbins, 1982). However, this definition requires instantaneously rapid mixing within the mixed layer. In systems with finite mixing rates the time resolution is shorter than this whereas in systems with advective feeding and tracer selective feeding the time resolution is greater than this (Robbins, 1986).

The thickness of the mixed layer has most often been determined from examination of ^{210}Pb profiles (Robbins, 1978) although other radionuclide distributions have been used also. Figure 1 shows the distributions of excess ^{210}Pb ($^{210}\text{Pb}_{\text{XS}}$) and total Kjeldahl nitrogen (TKN) from a core collected from Station 83 in the central basin of Lake Erie (Fisher et al., 1982). It is apparent that the $^{210}\text{Pb}_{\text{XS}}$ profile is described well by the mixing model where the thickness of the mixed layer is determined by the zone of uniform $^{210}\text{Pb}_{\text{XS}}$ activities and the sediment accumulation rate is determined from the exponential decrease in $^{210}\text{Pb}_{\text{XS}}$ activities in the undisturbed zone below.

However, the TKN profile appears transparent to mixing. Indeed, in the absence of the $^{210}\text{Pb}_{\text{XS}}$ data, one would assume that the sediment is unmixed. This apparent discrepancy is caused by differences in the relative magnitudes of the time-varying TKN depositional flux, the sedimentation rate, the rate and depth of bioturbation, and the rate of post-depositional decomposition of TKN. If the rate of TKN decomposition is slow relative to the rate of mixing (i.e., long half life) and the depositional flux of TKN is constant in time, then the TKN profile will look like that of ^{210}Pb . However, if the rate of TKN decomposition is rapid relative to the rate of mixing (i.e., short half life) and/or if the depositional flux increases with time then TKN will undergo a considerable downcore decrease and will appear transparent to mixing as in Figure 1. Failure to recognize post-depositional TKN degradation can lead to considerable error in interpretation of historical depositional fluxes and lake loadings (Fisher, et al., 1982).

Recently, stable isotopic analyses of organic matter in sediments have been used to reconstruct historical eutrophication and lake productivity of Lake Erie and Lake Ontario (Schelske and Hodell, 1991,1995; Henry et al., 1995; Eadie et al., 1995). These authors interpret downcore changes in the $\delta^{13}\text{C}$ and $\delta^{15}\text{N}$ and various phosphorus forms as evidence of past changes in the trophic status of the lakes. They report changes associated with forest clearing and early settlement, the eutrophication of the lakes from the 1940's-1970's, and improved water quality after the 1970's in response to phosphorus abatement programs. Their data suggest that events that occur over several years or longer can be resolved, and they indicate that there may be evidence that some events that occur over time periods of as little as a season may be identifiable. However, recent work has also shown that the infaunal benthic community in the lake is

capable of thoroughly mixing the sediment on a time-scale that is rapid with respect to the sedimentation rate (McCall and Fisher, 1980; Robbins, 1986; Robbins et al., 1989). This would imply that sediment profiles should be well mixed and not show evidence of short-term variations in the depositional flux of contaminants. This work addresses this apparent discrepancy between high resolution historical records derived from downcore sediment contaminant concentrations with sediments that are biologically mixed.

SEDIMENTATION RATES

Most of the earliest measurements of sedimentation rates in Lake Erie were based on palynology. Kemp et al. (1972; 1977) and Robbins et al. (1978) determined the depth of rapid increase in the abundance of *Ambrosia* pollen and calculated a sedimentation rate by assuming that the increase occurred due to clear cutting of the forests in about 1850 (Table 1). The linear sedimentation rate is calculated as the depth of the pollen change divided by the years since 1850 (cm/yr). The mass sedimentation rate is calculated as the cumulative mass of sediment above the depth of the pollen change (g/cm^2) divided by the years since 1850 ($\text{g}/\text{cm}^2/\text{yr}$). The linear sedimentation rate is related to the mass sedimentation rate by

$$\omega = \frac{r_s}{\rho_s(1 - \phi)} \quad (1)$$

where ω is the linear sedimentation rate (cm/yr), r_s is the mass sedimentation rate ($\text{g}/\text{cm}^2/\text{yr}$), ρ_s is the sediment bulk dry density $\approx 2.5 \text{ g}/\text{cm}^3$, and ϕ is the

porosity. The mass sedimentation approach accounts for sediment compaction, but neither method permits an evaluation of the time resolution.

Downcore measurements of radionuclides has become the most important method for determining sedimentation rates. Of particular interest is ^{210}Pb , because its 22.26 yr half life is ideally suited for establishing a geochronology for the past 100 yrs, mixing depths and time resolution can be inferred from its downcore distribution, and analysis by beta spectroscopy of its ^{210}Bi daughter (Jaworowski, 1969; Matsumoto, 1975), direct gamma spectroscopy (Cutshall et al., 1983; Schelske, et al., 1994), or alpha spectroscopy of its ^{210}Po granddaughter (Jaworowski, 1969; Turekian et al., 1973) are relatively routine. Although the alpha spectroscopic method has traditionally produced the most accurate results, the most popular method today is measurement of the 46.5 keV γ ray of ^{210}Pb decay because sample preparation is simple and non-destructive and total ^{210}Pb and ^{226}Ra (an estimate of supported ^{210}Pb) and ^{137}Cs (an independent time marker) are all determined simultaneously. However, as will be discussed below, different models for the interpretation of ^{210}Pb data result in different interpretations of the sedimentation rates and mixing depths.

Krishnaswami et al. (1971) applied the ^{210}Pb method to lake sediments and Robbins (1978) discusses in detail the application and interpretation of ^{210}Pb data in mixed sediments. However, a brief summary of the ^{210}Pb dating methodologies is useful for this work. ^{210}Pb is a natural decay product of the ^{238}U decay series. Its precursor, ^{226}Ra (1622 yr half-life) is distributed in rocks

and decays to gaseous ^{222}Rn (3.8 d half-life). Some of the ^{222}Rn escapes into the atmosphere, where it undergoes a series of very short-lived decays to ^{210}Pb . ^{210}Pb sorbes onto fine particulates and is scrubbed from the atmosphere in rainfall. Eventually these particles are incorporated into the sediments where the ^{210}Pb remains strongly sorbed to the particulates and is redistributed only by physical mixing. Because some ^{226}Ra is present in the sediment its decay produces some ^{210}Pb *in situ*. This portion of ^{210}Pb is called ‘supported ^{210}Pb ’ while the atmospherically-derived ^{210}Pb is called ‘unsupported’ or ‘excess ^{210}Pb ’ and their sum is the ‘total ^{210}Pb ’. Upon burial the ^{210}Pb undergoes decay; with uniform, continuous burial and no compaction $^{210}\text{Pb}_{\text{XS}}$ activity decreases exponentially downcore where it asymptotically approaches a constant supported ^{210}Pb value.

There are two models for calculating dates from ^{210}Pb core data (Robbins, 1978). One model, the constant activity (CA) or constant initial concentration (CIC) model assumes that the activity of ^{210}Pb in sediments accumulating at the sediment-water-interface is a constant (Krishnaswami et al., 1971). As the sedimentation rate increases, scavenging of ^{210}Pb from the water column increases. The constant flux (CF) or constant rate of supply (CRS) model assumes that the flux of ^{210}Pb to the sediment surface is constant and is independent of the sedimentation rate (Appleby and Oldfield, 1978;1983). If the sedimentation rate increases the activity of ^{210}Pb in sediment delivered to the

sediment-water interface decreases but the flux remains constant.

Downcore ages are calculated from the CIC model by

$$t = \lambda^{-1} \ln \frac{C(0)}{C(Z)} \quad (2)$$

where t =time (yr), λ = decay constant of ^{210}Pb ($= 0.03114 \text{ yr}^{-1}$), $C(0)$ is the specific activity of excess ^{210}Pb at the sediment-water interface (decays per min per gram dry sediment (dpm/g)), and $C(Z)$ is the specific activity of excess ^{210}Pb at depth Z (dpm/g)(Binford, 1990).

The CIC model fails if the ^{210}Pb activity-depth curve deviates from an exponential. Two examples of cases from Lake Erie where the model fails are shown in Figures 1 and 2. The profile in Figure 1 shows a surface, mixed zone in which the ^{210}Pb activity is constant. The CIC model can be modified to apply to these data, by assuming a two layer system in which mixing is expressed as an eddy diffusive process (Robbins, 1978). Ignoring compaction, assuming constant sedimentation, and assuming constant biodiffusion in the mixed layer, the ^{210}Pb activity, A , as a function of depth Z (cm) and time t (yr) is given by

$$\begin{aligned} \frac{\partial A}{\partial t} &= D_b \frac{\partial^2 A}{\partial Z^2} - \omega \frac{\partial A}{\partial Z} - \lambda A & 0 < Z \leq Z_m \\ \frac{\partial A}{\partial t} &= -\omega \frac{\partial A}{\partial Z} - \lambda A & Z > Z_m \end{aligned} \quad (3)$$

where D_b is the bioturbation coefficient (cm^2/yr), ω is the sedimentation rate (positive downward) (cm/sec), λ is the decay coefficient for ^{210}Pb ($= 0.03114 \text{ yr}^{-1}$), and Z_m is the depth at the base of the mixed layer (cm). The time resolution can be approximated as the thickness of the mixed layer divided by the sedimentation rate

$$\tau (\text{yr}) = \frac{Z_m (\text{cm})}{\omega (\text{cm} / \text{yr})} = \frac{Z_m (\text{g}/\text{cm})^2}{\omega (\text{g} / \text{cm}^2 / \text{yr})} \quad (4)$$

where τ is the time resolution. In Table 1, estimates of the loss of time resolution range from 4-34 yrs, although some authors report that there is no mixed layer evident in their cores.

A second example where the CIC model fails is given in Figure 2, where the ^{210}Pb activity in a core from Cleveland Harbor has a constant value from 0-6 cm and from 8-14 cm. One interpretation is that the deeper constant activity sediment layer accumulated as a single episode, perhaps as a storm deposit or deposition associated with harbor channel dredging. Recently, discontinuous ^{210}Pb profiles have been interpreted as storm deposits in Lake Michigan (Hermanson and Christensen, 1991) and Lake Erie (Lick et al., 1994). The CIC model can be applied to these data for the intervals between deposition events, or, it can include them if a long time interval is considered.

Downcore ages of sediments calculated using the CRS model can be determined from the relationship

$$t = \lambda^{-1} \ln \frac{A(0)}{A(Z)} \quad (5)$$

where A is the total, integrated ^{210}Pb activity (dpm/cm^2) below depth Z, or

$$A(Z) = \int_0^\infty p C(Z) dx \quad (6)$$

and p is the amount of dry-phase sediment per unit volume of wet sediment (gds/cm^3 wet sediment)(Binford, 1990). Both compaction and changes in the sedimentation rate are accounted for by this formulation. One problem with this model is that the sedimentation rate is adjusted at every depth interval, so independent evidence is needed to verify the results. Although mixing can be included in the model, the lower boundary of the mixing zone must be set subjectively.

It appears that both models work in different systems. The CIC model has been applied successfully in large lakes and reservoirs while the CRS model works best in medium-sized or small lakes (Binford, 1984). Large lakes may have a large, excess supply of ^{210}Pb in the water column that can supply ^{210}Pb when additional sediment is input and still maintain a constant activity at the sediment surface. Conversely, in a smaller lake the total pool of ^{210}Pb may be smaller and easily scavenged from the water column leading to a continuous deficiency of ^{210}Pb in the water column. As a result, a greater input of sediment

to a smaller lake does not result in a greater depositional flux of ^{210}Pb .

Considerably more effort has been made to develop these general models in an effort to 'unmix' bioturbation and improve the time resolution for paleolimnological interpretation of Lake Michigan than for Lake Erie. Robbins and Edgington (1975) measured ^{210}Pb and ^{137}Cs profiles and found that some of the cores indicated no mixing while other cores showed evidence of surface mixing. They also demonstrated that the 1963 ^{137}Cs activity peak had moved downward a greater distance than it should have by burial alone, and interpreted this to mean that ^{137}Cs had been mixed downward by bioturbation. Christensen and Klein (1991) found similarly that mixing causes the record to be shifted downward and features, such as the onset of pollution, can mistakenly be interpreted as occurring earlier than they actually did. Christensen and co-workers have unmixed the Lake Michigan sediment record of ^{137}Cs , Pb, Zn, Cd, and PAHs by a matrix method (Christensen and Goetz, 1987; Fukumori et al., 1992), by frequency domain deconvolution (Christensen and Osuna, 1989), by the inverse Berger-Heath model (Christensen and Klein, 1991; Christensen and Zhang, 1993), and by polynomial curve fitting of the depositional flux of the tracer (Christensen and Karls, 1996). They found that some of these methods (matrix and frequency domain methods) are difficult to implement and may have certain other limitations such as limited time resolution (Christensen and Goetz, 1987; Fukumori et al., 1992), while other methods (inverse Berger-Heath method) were relatively easy to implement and provided reasonably accurate results (Christensen and Klein, 1991; Christensen and Zhang, 1993). Christensen and Karls (1996) recently improved the inverse Berger-Heath calculation methodology and found that for small mixing depths the curve-fitting correction

calculation methods were not needed, but for larger mixing depths time resolution can be improved by the technique. They report that for a conservative tracer the two methods yield similar results when the Peclet number, $Pe = z_m^2/(D_b \Delta t)$ is the same.

Variables that control the time resolution include the mixed depth, the biodiffusion coefficient, the sedimentation rate, and the time resolution and magnitude of the depositional signal. Good time resolution would be expected when the sedimentation rate is high, biodiffusion coefficient low, small mixed depth interval, and a large change in the magnitude of the depositional signal. Conversely, a small rate of sediment accumulation, large biodiffusion coefficient, large mixing zone, and a small change in the magnitude of the depositional signal will lead to poor time resolution. An example of a case with excellent time resolution is given in Figure 3. The ^{137}Cs data from a 2 m core from Oahe Reservoir (Callender and Robbins, 1993) shows clearly identifiable annual signals. Also shown are monthly atmospheric fluxes recorded in Vermillion, South Dakota (Health and Safety Laboratory, 1977) for comparison with the core data. The annual signal is well preserved in the sediment because the sedimentation rates are so high (~10 cm/yr). In the Great Lakes few environments are likely to exhibit such high sedimentation rates (Table 1), although some nearshore, river mouths (estuaries), or harbor areas might.

Shelske and Hodell (1995) interpreted downcore oscillations of $\delta^{13}\text{C}_{\text{org C}}$ as annual or interannual changes in the depositional signal of organic carbon (Figure 4). They attributed the sawtooth pattern in the isotopic signature to changes in primary production and inorganic carbonate precipitation brought about by changes in climate and/or major ecosystem changes. Others have also claimed to have resolved events that occur over several years or longer, and

indicate that there may be evidence of some events that occur over time periods of as little as a season may be identifiable (Henry et al., 1995; Eadie et al., 1995). These recent claims of time resolutions from seasonal to several years are significantly shorter than those given by workers who report mixing depths (Table 1). The simulations below are designed to establish the time resolution possible in Lake Erie sediments under different mixing and chemical loading conditions.

SIMULATIONS

The time resolutions reported in Table 1 coupled with observations by several authors that some ^{210}Pb activity profiles decrease exponentially from the surface with no evidence of mixing, demonstrate that reported time resolutions range from <1 yr to several decades. Here some simulations of the simple 2-layer model (Eq. 3) are performed to illustrate the nature of the loss of time resolution caused by mixing, and how variations in the mixed depth interval, the biodiffusion coefficient, sedimentation rate, and tracer half life affect the recorded signal. The purpose of these simulations is not to present an improved method for calculating the time resolution, but rather to identify conditions in which annual or interannual changes in lake productivity or water quality can be expected to be identifiable in the sediment record.

Based on the data in Table 1 the parameter ranges considered in the simulations are 0.03-1 g/cm²/yr sedimentation rate, 0.1-200 cm²/yr biodiffusion coefficient, 1-8 cm mixed depth, 1-5 yr time varying depositional cycle, and 10 - 100% difference in the magnitude of the depositional signal. The numerical simulations were solved using a fully implicit finite difference approximation with $\Delta z=0.005$ cm, $\Delta t=0.01$ yr, total depth interval simulated = 50 cm, and total

time of simulation = 50 yr. These equations, when solved by this technique are well known to cause significant numerical dispersion, so the 'no mixing' (i.e., $D_b=0$) situation is shown in each case to permit visualization of the numerical dispersion in each instance. The value of the numerical dispersion coefficient was calculated from the rate of change of the square of the peak broadening in the 'no mixing' simulations and found to be $1.250 \times 10^{-2} \text{ cm}^2/\text{yr}$ - too large to permit interpretation of some data, but small relative to coefficients determined from most Lake Erie settings. In all 176 simulations were conducted. Shown here are selected results in which the mixed depth, biodiffusion coefficient, sediment accumulation rate, and duration and magnitude of the signal are varied, and how those parameters will be manifested in the ^{210}Pb and ^{137}Cs profiles. Figures 5-7 illustrate the effects of mixing depth, mixing rate, and tracer half-life on excess ^{210}Pb profiles and Figures 8-11 illustrate the effects of a time varying input and the magnitude of the input on tracer profiles.

The effect of mixing depth is illustrated in Figure 5, in which profiles of the relative activity of excess ^{210}Pb are shown for mixing depths from 1-8 cm. Compared to the non-mixing case, mixing causes activities to be higher within the mixed zone as well as everywhere below the mixed zone. In addition, this effect is greater with deeper mixing. This occurs because mixing removes some higher activity material from the surface and places it at the base of the mixed interval. This material is new and has not undergone decay while sediment from the same depth in the non-mixing case has slowly been buried to that depth and has experienced some decay. Also, rapid, shallow mixing (i.e., 1 cm) cannot be readily distinguished from the non-mixing case, although deep mixing should be readily identifiable in sampled cores.

The effect of the biogenic diffusion coefficient, D_b , is illustrated in Figure 6. For small values of D_b ($D_b \leq 1 \text{ cm}^2/\text{yr}$) the effect of mixing on excess ^{210}Pb profiles is negligible. Larger values of D_b ($D_b \geq 10 \text{ cm}^2/\text{yr}$) yield a well-defined mixed layer overlying sediment undergoing burial and decay. Larger biodiffusion coefficients result in higher activities in the sediment. This occurs because larger biodiffusion coefficients result in greater downward mixing of higher activity surface sediment. 'Typical' values for D_b estimated from oceanic, coastal marine and Great Lakes sediments range from 0.01-10 cm^2/yr . In the Great Lakes values for D_b average about 0.1 cm^2/yr , significantly less than that required to create a uniformly mixed surface layer. Consequently, the time resolution of a signal as it is transported through the mixed layer by burial is less than that calculated from Eqn. (4).

In the discussion of Fig. 1 the question was posed why some parameters such as TKN appear to be transparent to mixing while other parameters, such as ^{210}Pb , show a mixed surface layer. Insight to this phenomenon can be seen in Figure 7, where downcore profiles are calculated for tracers of varying half lives. Tracers with very long half-lives undergo little decay, so that their downcore profiles exhibit conservative behavior and do not appear mixed if the surface concentration remains constant. Tracers with short half-lives undergo significant decay during residence in the mixed layer, so that their concentrations decrease rapidly downcore and their profiles show no evidence of mixing. Variations in the tracer half-life result in significant differences in their downcore profiles. For ^{210}Pb or ^{137}Cs dating of sediment this effect is irrelevant because the tracer half-life is known precisely. However, organic contaminants exhibit a wide range of half-lives. Their downcore profiles would

be expected to vary widely and are controlled not only by their historical loadings, but also by their degradation rates.

The effect of mixing depth is illustrated in Figures 8 and 9. Mixing causes peaks to be mixed downward and appear lower in the sediment column than in the absence of mixing. This causes events to be interpreted as occurring earlier than they actually did. It also results in prolonged retention of 'buried' sediment in the surface zone so that events appear to persist longer than they actually did. The greater the mixing depth or the greater the bioturbation coefficient the greater the downward shift of the peaks and the greater the retention in the mixed zone, but the greater the destruction of the signal. When there is a large difference in the depositional signal, very rapid deep mixing leads to homogenization of the signal, but it is still identifiable. A 10% change in the signal is barely perceptible even in the absence of mixing and with mixing the sediment is completely homogenized to the long-term mean value. The effect of the diffusion coefficient makes little difference to the mixing profiles. The mixing depth and sedimentation rates are more important variables for the range of parameter coefficients typical of Lake Erie.

The effect of the rate of sediment accumulation is illustrated in Figures 10 and 11 for variations of 1-5 years in the input signal. Rapid rates of sediment accumulation favor preservation of the input signal, even with rapid, deep mixing. Annual signals are readily identified when sedimentation rates are as high as 3 cm/yr. However, when sedimentation rates are much less (~0.1 cm/yr) there is total loss of signal resolution and the tracer concentrations equal the long-term mean. However, even with significant loss of signal resolution sedimentation rates determined from ^{210}Pb and ^{137}Cs can be readily determined. The atmospheric flux of ^{137}Cs to the Great Lakes is slightly

different than the flux recorded in South Dakota (Figure 3), but the essential features remain the same: interannual fallout maxima occurred in 1958, 1963, 1970, and 1974. These interannual peaks separated by 4-7 years can be readily identified when the sedimentation rate is high and the mixing is not too deep or vigorous. However, deep, vigorous mixing and low sedimentation rates result in the homogenization of the ^{137}Cs flux and permit the identification of only a single peak. This peak is usually assigned a date of 1963 and sedimentation rates are calculated based on its depth in the sediment. As noted above, mixing results in a downward shift of the peaks, causing the ^{137}Cs peak to appear up to several cm deeper than in the absence of mixing. This results in overestimating recent sedimentation rates and assigns an older date to the sediment than it is.

CONCLUSIONS

Several general conclusions about the resolution of downcore sediment profiles can be reached from this survey of existing data sets and computer simulations of sediment mixing. Mixing causes tracer concentrations to be higher in the sediment because of downward transport from the surface layers to the base of the mixing zone. This effect is greater with deeper mixing. Mixing also causes a downward shift of the sediment, so that a time tracer will appear deeper in the sediment in the presence of mixing than in its absence. For an instantaneously, homogeneously mixed layer, this downward shift is equal to the thickness of the mixed layer and the loss of time resolution is given by Equation (4). Using 'typical' values for the sedimentation rate in Lake Erie (0.1-1 cm/yr) and the mixed depth (1-8 cm) this yields a loss in time resolution ranging from 1-80 years, with most estimates falling in the 10-30 year range. However, the assumptions used in Equation (4) overestimate the loss in time resolution

because the surface sediment layer is not uniformly and instantaneously mixed so that tracer profiles are not completely homogenized and the preservation of even a portion of a time varying signal can be used to distinguish sediment of different ages. Identification of small, temporal variations in the magnitude of a sediment input signal in deep, actively mixed sediments is impossible.

However, in some areas where the sedimentation rate is high and bioturbation is not too deep or vigorous, it is possible to distinguish between sediments tagged with small differences in the input signal. In Lake Erie, interannual differences of 3-7 years can be readily identified in some locations, but it is still unclear if annual changes can be identified.

The downward transport of sediment because of mixing leads to inaccurate sediment dating. If mixing moves sediment downward by only 2 cm, at a sedimentation rate of 0.1 cm/yr this amounts to a 20 year error in the date of that layer and represents a 10% error in the sedimentation rate determined over a 20 cm sediment column.

The profiles of some substances are transparent to mixing while other parameters display well-mixed profiles. If the residence time of a sediment parameter in the mixed layer is long relative to the rate of decay or decomposition of the parameter, then the parameter will decrease throughout the mixed layer and its profile will not indicate that there is mixing. On the other hand, if the residence time of the parameter in the mixed layer is short relative to its rate of decay then a well defined mixed layer will appear. In addition, the depth of the deepest mixing will be apparent, so that less frequent, deep mixing events will only be identifiable from tracer profiles with longer half-lives. If the half-life is long relative to the rate of burial, the parameter will exhibit conservative behavior and there will be little change in its downcore profile regardless of mixing.

ACKNOWLEDGEMENTS

This work was supported by Lake Erie Protection Fund Small Grant SG 15/95.

REFERENCES

- Appleby, P.G. and F. Oldfield, 1978. The calculation of lead-210 dates assuming a constant rate of supply of unsupported ^{210}Pb to the sediment. *Catena* **5**:1-8.
- Appleby, P.G. and F. Oldfield, 1983. The assessment of ^{210}Pb data from sites with varying sediment accumulation rates. *Hydrobiologia* **103**:29-35.
- Berger, W.H. and G.R. Heath, 1968. Vertical mixing in pelagic sediments. *J. Mar. Res.* **26**:134-143.
- Binford, M.W., 1984. Dating lake sediment cores with ^{210}Pb . In *Paleolimnological Studies of the History and Effects of Acidic Precipitation* (S.A. Norton, ed.), pp.17-33, Proceedings of a Workshop on Paleolimnological Studies of the History and Effects of Acidic Precipitation, U.S. EPA Project #CR-811631-01-0.
- Binford, M.W., 1990. Calculation and uncertainty analysis of ^{210}Pb dates for PIRLA project lake sediment cores. *J. Paleolim.* **3**:253-267.
- Callender, E. and J.A. Robbins, 1993. Transport and accumulation of radionuclides and stable elements in a Missouri River reservoir. *Wat. Resour. Res.* **29**:1787-1804.
- Christensen, E.R. and R.H. Goetz, 1987. Historical fluxes of particle-bound pollutants from deconvolved sedimentary records. *Environ. Sci. Technol.* **21**:1088-1096.

- Christensen, E.R. and J. Osuna, 1989. Atmospheric fluxes of lead, zinc, and cadmium from frequency domain deconvolution of sedimentary records. *J. Geophys. Res.* **94**:14,585-14,597.
- Christensen, E.R. and R.J. Klein, 1991. "Unmixing" of ^{137}Cs , Pb, Zn, and Cd records in lake sediments. *Environ. Sci. Technol.* **25**:1627-1637.
- Christensen, E.R. and J.F. Karls, 1996. Unmixing of lead, ^{137}Cs , and PAH records in lake sediments using curve fitting with first-and second-order corrections. *Wat. Res.* **30**:2543-2558.
- Christensen, E.R. and X. Zhang, 1993. Sources of polycyclic aromatic hydrocarbons to Lake Michigan determined from sedimentary records. *Environ. Sci. Technol.* **27**:139-146.
- Cutshall, N.H., I.L. Larsen, and C.R. Olsen, 1983. Direct analysis of ^{210}Pb in sediment samples: self-absorption corrections. *Nuclear Instr. Meth.* **206**:309-312.
- Davis, R.B., 1974. Stratigraphic effects of tubificids in profundal lake sediments. *Limnol. Oceanogr.* **19**:466-488.
- Eadie, B.J., M.B. Lansing, and J.A. Robbins, 1995. Records of ecosystem changes in the isotope signatures of organic matter in Great Lakes cores. p. 73, 38th Conference of the International Association for Great Lakes Research, East Lansing, MI (Abstract).
- Fisher, J.B., G. Matisoff, and W.J. Lick, 1982. Downcore variation in sediment organic nitrogen. *Nature* **296**:345-347.
- Frederick, V.R, 1981. Primary investigation of the algal flora in the sediments of Lake Erie. *J. Great Lakes Res.* **7**:404-408.
- Fukumori, E., E.R. Christensen, and R.J. Klein, 1992. A model for ^{137}Cs and other tracers in lake sediments considering particle size and the inverse

- solution. *Earth Planet. Sci. Lett.* **11**:485-99.
- Goldberg, E.D., and M. Koide, 1962. Geochronological studies of deep sea sediments by the ionium/thorium method. *Geochem. Cosmochim. Acta* **26**:417-450.
- Health and Safety Laboratory, 1977. Final tabulation of monthly ^{90}Sr fallout data: 1954-1976. *Environ. Q.* HASL-329, 401pp., Dep. of Energy, New York.
- Henry, J. P. Ostrom, N. Ostrom, B. Eadie, and P.A. Meyers, 1995. Compound specific carbon isotopic evidence of the historical eutrophication of Lake Erie. p. 74, 38th Conference of the International Association for Great Lakes Research, East Lansing, MI (Abstract).
- Hermanson, H.H. and E.R. Christensen, 1991. Recent sedimentation in Lake Michigan. *J. Great Lakes Res.* **17**:33-50.
- Jaworowski, Z., 1969. Radioactive lead in the environment and in the human body. *Atom. Energy Rev.* **7**:3-45.
- Kemp, A.L.W., C.B.J. Gray, and A. Mudrochova, 1972. Changes in C,N,P, and S in the last 140 years in three cores from lakes Ontario, Erie, and Huron. In *Nutrients in Natural Waters* (H.E. Allen and J.R. Kramer, eds.) pp.251-279, Wiley, New York.
- Kemp, A.L.W., G.A. MacInnis and N.S. Harper, 1977. Sedimentation rates and a revised sediment budget for Lake Erie. *J. Great Lakes Res.* **3**:221-233.
- Krishnaswami, S. D. Lal, J.M.Martin, and M. Meybeck, 1971. Geochronology of lake sediments. *Earth Planet. Sci. Lett.* **11**:407-414.
- Lick, W., J. Lick, and C.K. Ziegler, 1994. The resuspension and transport of fine-grained sediments in Lake Erie. *J. Great Lakes Res.* **20**:599-612.
- Matisoff, G. and G.R. Holdren Jr., 1995. A model for sulfur accumulation in soft water lake sediments. *Water Resour. Res.* **31**:1751-1760.
- Matsumoto, E., 1975. Pb-210 geochronology of sediments from Lake Sinji.

- Geochem. J. **9**:167-172.
- McCall, P.L. and J.B. Fisher, 1980. Effects of tubificid oligochaetes on physical and chemical properties of Lake Erie sediments. In *Aquatic Oligochaete Biology* (R.O. Brinkhurst and D.G. Cook, eds.) pp.253-318, Plenum Press, New York, NY.
- Nriagu, J.O., A.L.W. Kemp, H.K.T.Wong, and H.Harper, 1979. Sedimentary record of heavy metal pollution in Lake Erie. *Geochem. Cosmochim. Acta* **43**:247-258.
- Robbins, J.A., 1978. Geochemical and geophysical applications of radioactive lead. In *Biogeochemistry of Lead in the environment* (J.O. Nriagu, ed.) pp.285-393, Elsevier, Amsterdam.
- Robbins, J.A., 1982. Stratigraphic and dynamic effects of sediment reworking by Great Lakes zoobenthos. *Hydrobiologia* **92**:611-622. Reprinted in *Developments in Hydrobiology: Sediment-Freshwater Interaction* (P.G. Sly, ed.) W. Junk, Boston.
- Robbins, J.A., 1986. A model for particulate-sediment transport of tracers in sediments with conveyor-belt deposit feeders. *J. Geophys. Res.*, **91**:8542-8558.
- Robbins, J.A. and D.N. Edgington, 1985. Determination of recent sedimentation rates in Lake Michigan using Pb-210 and Cs-137. *Geochem. Cosmochim. Acta* **39**:285-304.
- Robbins, J.A., D.N. Edgington, and A.L.W. Kemp, 1978. Comparative ^{210}Pb , ^{137}Cs , and pollen geochronologies of sediments from Lakes Ontario and Erie. *Quaternary Res.* **10**:256-278.
- Robbins, J.A., T. Keilty, D.S. White, and D.N. Edgington, 1989. Relationships among tubificid abundances, sediment composition, and accumulation

- rates in Lake Erie. *Can. J. Fish. Aquatic. Sci.* **46**: 223-231.
- Schelske, C.L. and D.A. Hodell, 1991. Recent changes in productivity and climate of Lake Ontario detected by isotopic analysis of sediments. *Limnol. Oceanogr.* **36**:961-975.
- Schelske, C.L. and D.A. Hodell, 1995. Using carbon isotopes of bulk sedimentary organic matter to reconstruct the history of nutrient loading and eutrophication in Lake Erie. *Limnol. Oceanogr.* **40**:918-929.
- Schelske, C.L. A. Peplow, M. Brenner, and C.N. Spencer, 1994. Low-background gamma counting: applications for ^{210}Pb dating of sediments. *J. Paleolimnol.* **10**:115-128.
- Turekian, K.K., D.P. Kharkar, and J. Thomson, 1973. Uranium and thorium decay series nuclide abundances in marine plankton. Final Report, Advanced Res. Proj. Agency, Order No. 1793, Contract NOOO14-67-A-0097-0022, Yale University, New Haven, Conn.

FIGURE CAPTIONS

Figure 1. Downcore concentrations of total Kjeldahl nitrogen (TKN) and excess ^{210}Pb from station 83 in the central basin of Lake Erie. Note that the $^{210}\text{Pb}_{\text{XS}}$ activity is constant over the top 4.5 cm mixed layer whereas the TKN concentration decreases rapidly throughout that zone.

Figure 2. Downcore activities of total ^{210}Pb in a core from Cleveland Harbor. The ^{210}Pb activity decreases exponentially from 6-8 cm and at depths greater than 14 cm. The constant value from 8-14 cm may be interpreted as sediment accumulation from a single episode, perhaps as a storm deposit.

Figure 3. Downcore activities of ^{137}Cs in a core from Oahe Reservoir, S.D. (data from Callender and Robbins, 1993) correlated with monthly averaged atmospheric fallout monitoring data from Vermillion, S.D. (data from Health and Safety Laboratory, 1977). The relatively large and small seasonal atmospheric fluxes of ^{137}Cs can be correlated with annual signals of ^{137}Cs activity in the sediment. The large ^{137}Cs fallout during the early 1960's caused by nuclear weapons testing are well defined in the sediment as annual events even though the radionuclide is subject to some watershed retention.

Figure 4. Downcore concentrations of $\delta^{13}\text{C}$ in a core from the eastern basin of Lake Erie (data from Schelske and Hodell, 1995). Schelske and Hodell interpret the general trend of heavier carbon until 1970 and then lighter carbon after 1970 as changes caused by eutrophication and later by decreased phosphorus loading. They also attribute the oscillations in the

upper part of the column as interannual changes in productivity.

Figure 5. Simulated downcore activities of excess ^{210}Pb for 1, 3, and 8 cm mixing. Active mixing ($D_b=10 \text{ cm}^2/\text{yr}$), a constant sedimentation rate ($r_s=0.3 \text{ gds/cm}^2/\text{yr} \approx 1 \text{ cm/yr}$), a constant activity of tracer at the sediment-water interface and a half-life equal to that of ^{210}Pb (22.6 yr) assumed in all simulations. Note that deeper mixing results in higher tracer activities all all depths below the mixed zone.

Figure 6. Simulated downcore activities of excess ^{210}Pb for biogenic diffusion coefficients D_b from 0.1-200 cm^2/yr . A mixing depth = 8 cm, a constant sedimentation rate ($r_s=0.3 \text{ gds/cm}^2/\text{yr} \approx 1 \text{ cm/yr}$), a constant activity of the tracer at the sediment-water interface and a half-life equal to that of ^{210}Pb (22.6 yr) assumed in all simulations. Note that very active mixing ($D_b \geq 10 \text{ cm}^2/\text{yr}$) is needed to generate a sediment profile that exhibits an obvious mixed layer. More typical mixing rates of $D_b = 0.1-1 \text{ cm}^2/\text{yr}$ create excess ^{210}Pb profiles in which mixing appears small and may go undetected.

Figure 7. Simulated downcore activities of particle bound tracers with half-lives ranging from 0.1-100 yr. Active mixing ($D_b=10 \text{ cm}^2/\text{yr}$), a mixing depth = 8 cm, a constant sedimentation rate ($r_s=0.3 \text{ gds/cm}^2/\text{yr} \approx 1 \text{ cm/yr}$), and a constant activity of the tracer at the sediment-water interface assumed in all simulations. Note that a tracer with a very long half-life will exhibit behavior like that of a conservative component, and since its concentration at the sediment surface does not vary in time its concentration will not

decrease with depth in the sediment. A tracer with a very short half-life will undergo significant decay within the mixed zone and will appear transparent to mixing.

Figure 8. Effect of mixing depth on tracer preservation. $D_b=0.1 \text{ cm}^2/\text{yr}$ and $r_s=0.3 \text{ gds/cm}^2/\text{yr} \approx 1 \text{ cm/yr}$ used in all simulations. Upper left: numerical dispersion of a conservative tracer undergoing a 3 year oscillatory input signal; upper center: ^{210}Pb with 1 cm mixed layer; upper right: ^{137}Cs with 1 cm mixed layer; lower left: 3 yr oscillatory signal with 1 cm mixed layer; lower center: 3 yr oscillatory signal with 3 cm mixed layer; lower right: 3 yr oscillatory signal with 8 cm mixed layer.

Figure 9. Effect of mixing depth on tracer preservation. $D_b=1.0 \text{ cm}^2/\text{yr}$ and $r_s=0.3 \text{ gds/cm}^2/\text{yr} \approx 1 \text{ cm/yr}$ used in all simulations. Upper left: numerical dispersion of a conservative tracer undergoing a 10% 5 year variation in the magnitude of the input signal; upper center: ^{210}Pb with 8 cm mixed layer; upper right: ^{137}Cs with 8 cm mixed layer; lower left: 5 yr oscillatory signal with 1 cm mixed layer; lower center: 5 yr oscillatory signal with 3 cm mixed layer; lower right: 5 yr oscillatory signal with 8 cm mixed layer.

Figure 10. Effect of variations of the input signal time on tracer preservation. $D_b=0.1$, $r_s=1.0 \text{ gds/cm}^2/\text{yr} \approx 3 \text{ cm/yr}$, and mixing depth = 3 cm used in all simulations. Upper left: numerical dispersion of a conservative tracer undergoing a 3 year oscillatory input signal; upper center: ^{210}Pb ; upper right: ^{137}Cs ; lower left: 1 yr oscillatory signal; lower center: 3 yr

oscillatory signal; lower right: 5 yr oscillatory signal.

Figure 11. Effect of variations of the input signal time on tracer preservation.

$D_b=0.1$, $r_s=0.03$ gds/cm²/yr ≈ 0.1 cm/yr, and mixing depth = 3 cm used in all simulations. Upper left: numerical dispersion of a conservative tracer undergoing a 10% 3 year variation in the magnitude of the input signal; upper center: ²¹⁰Pb; upper right: ¹³⁷Cs; lower left: 1 yr oscillatory signal; lower center: 3 yr oscillatory signal; lower right: 5 yr oscillatory signal.

Table 1. Summary of Measurements of Present-Day Sediment Accumulation Rates (r_s), Mixing Depths (Z_m), and Time Resolutions (τ) in cores from Lake Erie.

Core ID	Location*	Dating Method [‡]	r_s (mg/cm ² /yr)	ω (cm/yr) [†]	Z_m (cm) [¶]	τ (yrs) [#]	Ref
K-30	EB	<i>Ambrosia</i>	8	0.03			2
K-31	EB	<i>Ambrosia</i>	8	0.03			2
K-32	EB	<i>Ambrosia</i>	14	0.05			2
L-28	EB	<i>Ambrosia</i>	150	0.38			2
L-29	EB	<i>Ambrosia</i>	314	0.41			2
L-30	EB	<i>Ambrosia</i>	93-124	0.25-0.34			2
L-31	EB	<i>Ambrosia</i>	30-42	0.10-0.13			2
M-30	EB	<i>Ambrosia</i>	>73	>0.22			2
M-31	EB	<i>Ambrosia</i>	278	0.66			2
M-32	EB	<i>Ambrosia</i>	269-379	0.65-0.85			2
M-32	EB	<i>Ambrosia</i>	270	0.85			3
M-32	EB	²¹⁰ Pb CIC	440	1.40			3
M-32	EB	¹³⁷ Cs	350	1.20			3
M-33	EB	<i>Ambrosia</i>	164	0.43			2
M-34	EB	<i>Ambrosia</i>	314-350	0.41-0.45			2
N-30	EB	<i>Ambrosia</i>	162-175	0.42-0.45			2
N-32	EB	<i>Ambrosia</i>	431	0.95			2
N-34	EB	<i>Ambrosia</i>	215.5	0.33			2
N-35	EB	<i>Ambrosia</i>	18	0.05			2
O-30	EB	<i>Ambrosia</i>	0.0	0.0			2
O-31	EB	<i>Ambrosia</i>	36	0.12			2
32	EB	<i>Ambrosia</i>	4	0.02			2
O-33	EB	<i>Ambrosia</i>	0.0	0.0			2
1A	EB	²¹⁰ Pb CIC	128	0.48			4
1B	EB	²¹⁰ Pb CIC	204	0.85			4
1C	EB	²¹⁰ Pb CIC	161	0.67			4
	EB	<i>Ambrosia</i>		0.205			5
33 (1976)	EB	²¹⁰ Pb CIC, ¹³⁷ Cs	10		0.34 η	34	6
38 (1976)	EB	²¹⁰ Pb CIC, ¹³⁷ Cs	570		3.81 η	7	6
38 (1978)	EB	²¹⁰ Pb CIC, ¹³⁷ Cs	860		5.20 η	6	6
42 (1976)	EB	²¹⁰ Pb CIC, ¹³⁷ Cs	450		1.84 η	4	6
42 (1978)	EB	²¹⁰ Pb CIC, ¹³⁷ Cs	330		2.18 η	7	6
LE-42-87	EB	²¹⁰ Pb CRS	300-800				7
LE-42-87	EB	¹³⁷ Cs	555				7
47 (1976)	EB	²¹⁰ Pb CIC, ¹³⁷ Cs	140		0.86 η	6	6
LE-47 (1987)	EB	²¹⁰ Pb CRS	250-440				7
LE-47 (1987)	EB	¹³⁷ Cs	369				7
LE-47 (1993)	EB	¹³⁷ Cs	420				7
52 (1976)	EB	²¹⁰ Pb CIC, ¹³⁷ Cs	240		0.92 η	4	6
55 (1976)	EB	²¹⁰ Pb CIC, ¹³⁷ Cs	80		0.49 η	6	6
58 (1976)	EB	²¹⁰ Pb CIC, ¹³⁷ Cs	40		0.66 η	17	6
LLS (1982)	EB	²¹⁰ Pb CIC, ¹³⁷ Cs	590		3.23 η	5	6
LS (1982)	EB	²¹⁰ Pb CIC, ¹³⁷ Cs	340		1.54 η	4	6
MS (1982)	EB	²¹⁰ Pb CIC, ¹³⁷ Cs	620		2.96 η	5	6

A-8	CB	<i>Ambrosia</i>	199	0.30			2
B-8	CB	<i>Ambrosia</i>	83	0.17			2
C-12	CB	<i>Ambrosia</i>	57	0.22			2
D-10	CB	<i>Ambrosia</i>	20	0.07			2
D-13	CB	<i>Ambrosia</i>	45	0.18			2
D-15	CB	<i>Ambrosia</i>	25	0.12			2
E-11	CB	<i>Ambrosia</i>	52.5	0.15			2
E-12	CB	<i>Ambrosia</i>	15	0.08			2
F-10	CB	<i>Ambrosia</i>	79	0.17			2
F-15	CB	<i>Ambrosia</i>	57	0.22			2
F-18	CB	<i>Ambrosia</i>	135-166	0.26-0.31			2
G-12	CB	<i>Ambrosia</i>	45	0.18			2
G-14	CB	<i>Ambrosia</i>	25	0.12			2
G-16 (1970)	CB	<i>Ambrosia</i>	54.0		2	0	1
G-16 (1971)	CB	<i>Ambrosia</i>	62	0.23			2
G-16 (1973)	CB	<i>Ambrosia</i>	>75	>0.26			2
G-16	CB	²¹⁰ Pb CIC	83	0.46			3
G-16	CB	¹³⁷ Cs	80	0.44			3
G-16	CB	<i>Ambrosia</i>	73	0.40			3
G16 (1982)	CB	²¹⁰ Pb CIC, ¹³⁷ Cs	100		1.20 η	12	6
H-18	CB	<i>Ambrosia</i>	80	0.18			2
H-21	CB	<i>Ambrosia</i>	55.5	0.08			2
H-24	CB	<i>Ambrosia</i>	14	0.03			2
I-23-1	CB	<i>Ambrosia</i>	35-55	0.11-.16			2
J-16	CB	<i>Ambrosia</i>	37	0.16			2
J-18	CB	<i>Ambrosia</i>	51	0.13			2
J-21	CB	<i>Ambrosia</i>	18	0.05			2
L-19	CB	<i>Ambrosia</i>	39.5	0.08			2
2A	CB	²¹⁰ Pb CIC	24	0.05			4
2B	CB	²¹⁰ Pb CIC	13	0.05			4
2C	CB	²¹⁰ Pb CIC	18	0.02			4
3A	CB	²¹⁰ Pb CIC	17	0.02			4
3B	CB	²¹⁰ Pb CIC	16	0.02			4
3C	CB	²¹⁰ Pb CIC	22	0.06			4
4A	CB	²¹⁰ Pb CIC	17	0.10			4
4B	CB	²¹⁰ Pb CIC	24	0.12			4
4C	CB	²¹⁰ Pb CIC	18	0.15			4
5A	CB	²¹⁰ Pb CIC	41	0.25			4
5B	CB	²¹⁰ Pb CIC	22	0.16			4
5C	CB	²¹⁰ Pb CIC	36	0.19			4
6B	CB	²¹⁰ Pb CIC	22	0.15			4
6C	CB	²¹⁰ Pb CIC	13	0.06			4
GASP-83	CB	²¹⁰ Pb CIC	77	0.168	4.5/1.2 δ	16	8
	CB	²¹⁰ Pb CIC	96	0.23	0.0		9
30 (1976)	CB	²¹⁰ Pb CIC, ¹³⁷ Cs	30		0.22 η	7	6
10 (1976)	CB	²¹⁰ Pb CIC, ¹³⁷ Cs	70		1.48 η	21	6
24 (1976)	CB	²¹⁰ Pb CIC, ¹³⁷ Cs	50		0.95 η	19	6
13 (1976)	CB	²¹⁰ Pb CIC, ¹³⁷ Cs	20		0.40 η	24	6
16 (1976)	CB	²¹⁰ Pb CIC, ¹³⁷ Cs	20		0.35 η	18	6

20 (1976)	CB	^{210}Pb (CIC), ^{137}Cs	60		0.71 η	12	6
28 (1976)	CB	^{210}Pb CIC, ^{137}Cs	30		0.63 η	21	6

F-4	WB	<i>Ambrosia</i>	213		0.35		2
U-41	WB	<i>Ambrosia</i>	434-484		0.66-0.71		2
U-42 (1971)	WB	<i>Ambrosia</i>	160		0.30		2
U-42 (1975)	WB	<i>Ambrosia</i>	59-93		0.11-0.17		2
V-43	WB	<i>Ambrosia</i>	24-44		0.05-0.10		2
W-41	WB	<i>Ambrosia</i>	>645		>0.74		2
W-44	WB	<i>Ambrosia</i>	>151		>0.26		2
U-42	WB	^{210}Pb CIC	96		0.20		3
U-42	WB	^{137}Cs	47		0.10		3
U-42	WB	<i>Ambrosia</i>	59		0.12		3
7A	WB	^{210}Pb CIC	76		0.27		4
7B	WB	^{210}Pb CIC	92		0.33		4
7C	WB	^{210}Pb CIC	109		0.39		4
6 (1976)	WB	^{210}Pb CIC, ^{137}Cs	120			1.45 η	12

C-5	Islands	<i>Ambrosia</i>	135		0.26		2
T-44	Islands	<i>Ambrosia</i>	84		0.11		2
Cleveland	Harbor	^{210}Pb CIC	180/300 γ		0.19/0.33 γ	5.0	15/26

* EB = Eastern Basin; CB = Central Basin; WB = Western Basin

‡ CIC = Constant Initial Concentration Model (Robbins and Edgington, 1975); CRS = Constant Rate of Supply Model (Appleby and Oldfield, 1978)

$\omega = r_s / (1-\phi)\rho_s$ where ϕ is the porosity and ρ_s is the sediment bulk dry density $\approx 2.6 \text{ g/cm}^3$

$\eta \text{ g/cm}^2$ for data from Robbins et al., 1989 (Ref#6)

$\tau = Z_m / \omega$

$\delta \text{ g/cm}^2$

γ Sedimentation rates also calculated including 6 cm depositional event from 8 cm - 14 cm

1 Kemp et al., 1972

2 Kemp et al., 1977

3 Robbins et al., 1978

4 Nriagu et al., 1979

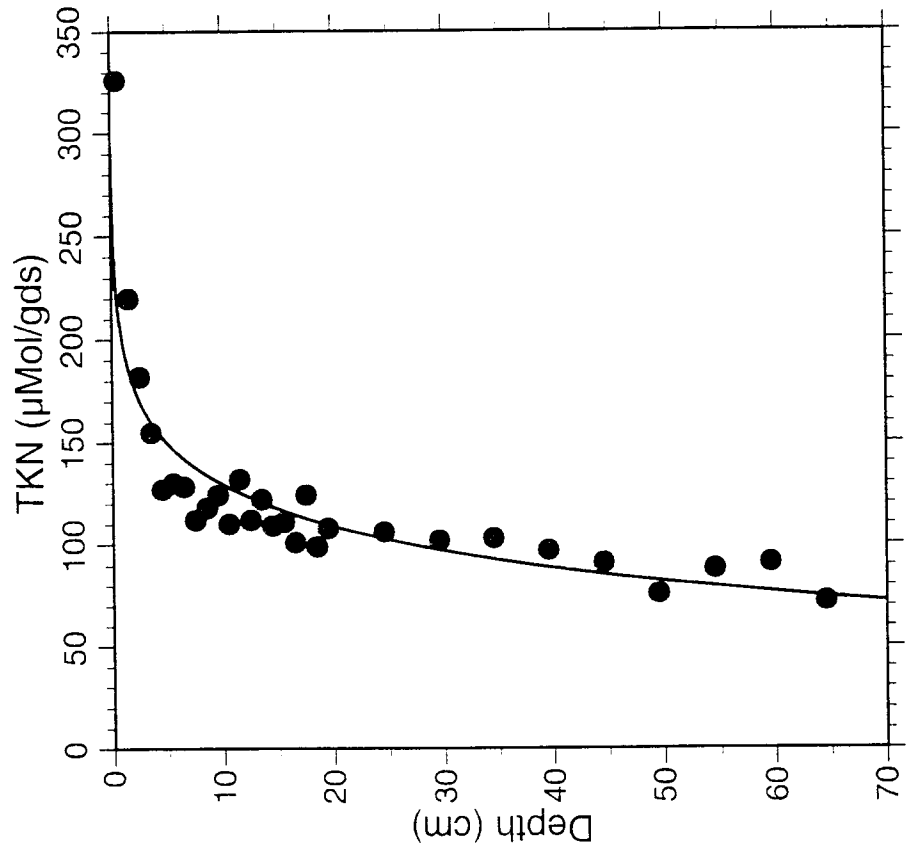
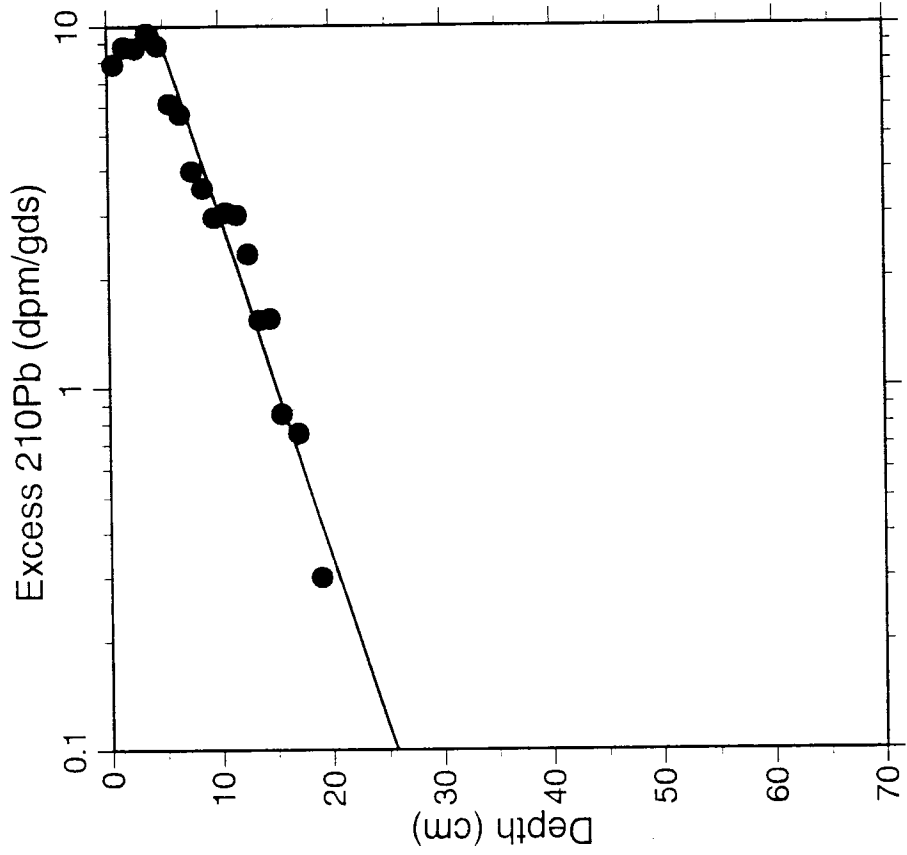
5 Frederick, 1981

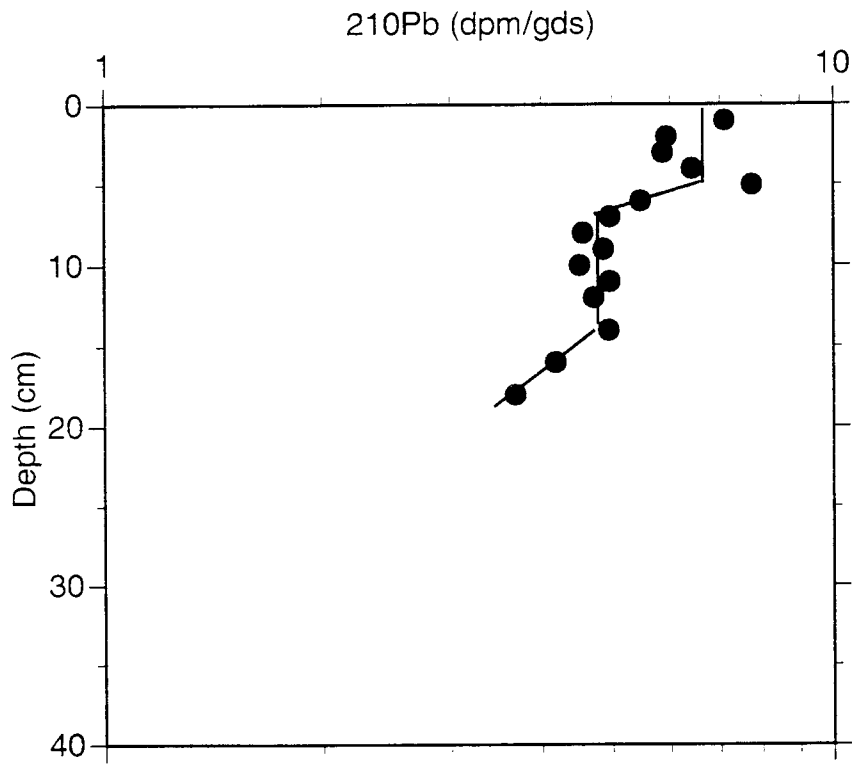
6 Robbins et al., 1989

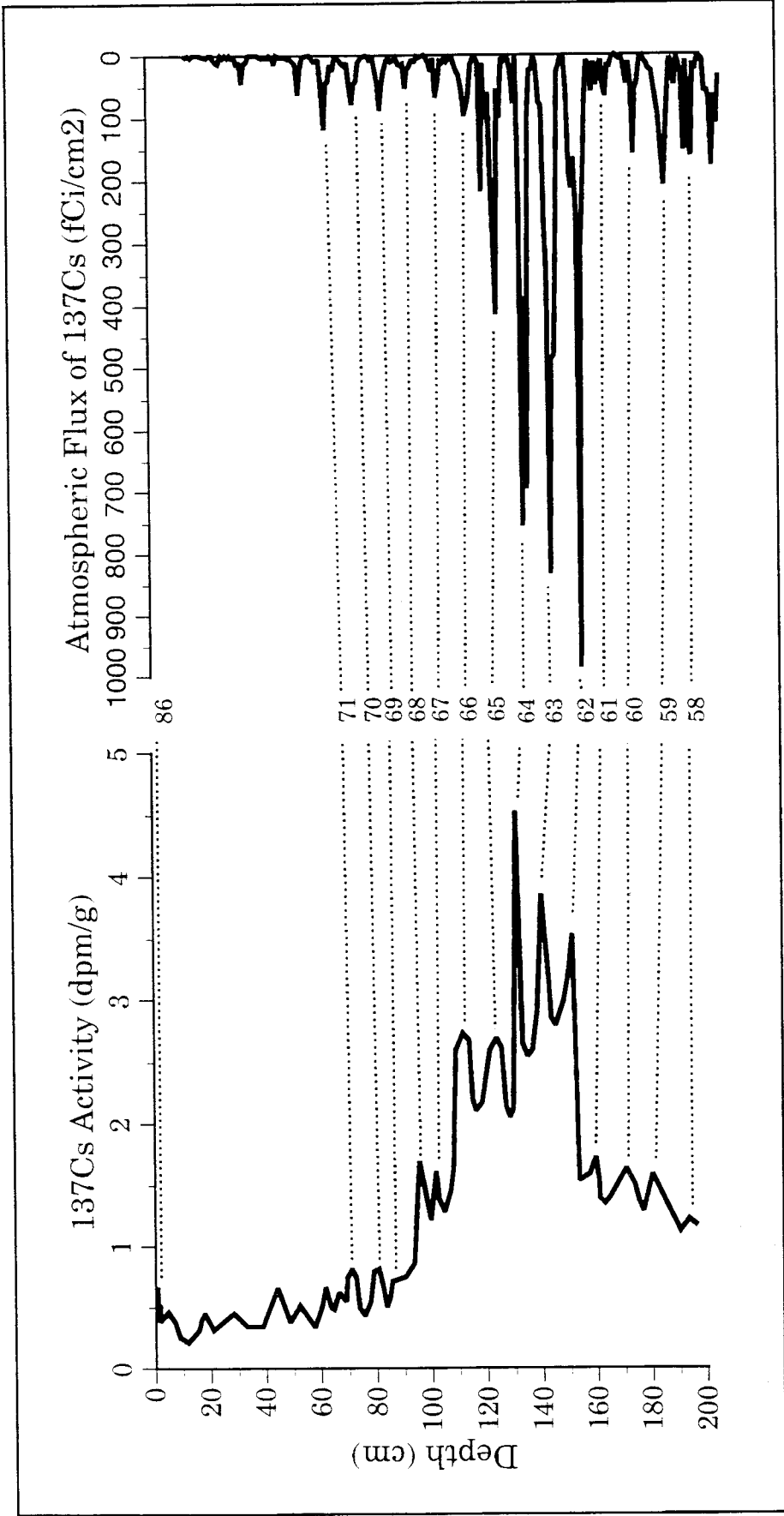
7 Schelske and Hodell, 1995

8 Robbins, unpublished data

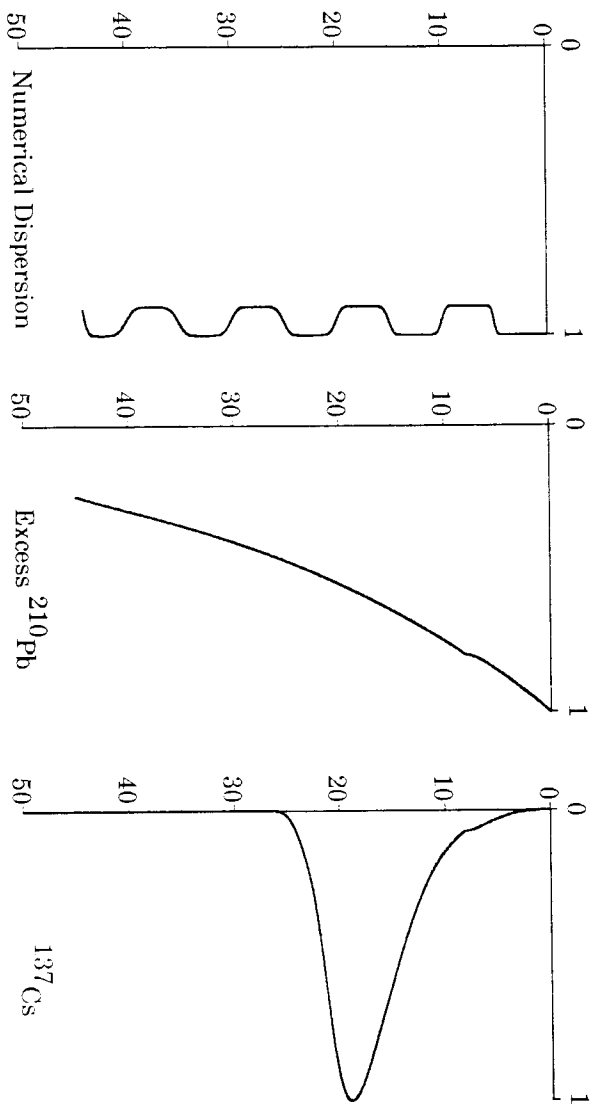
9 This work



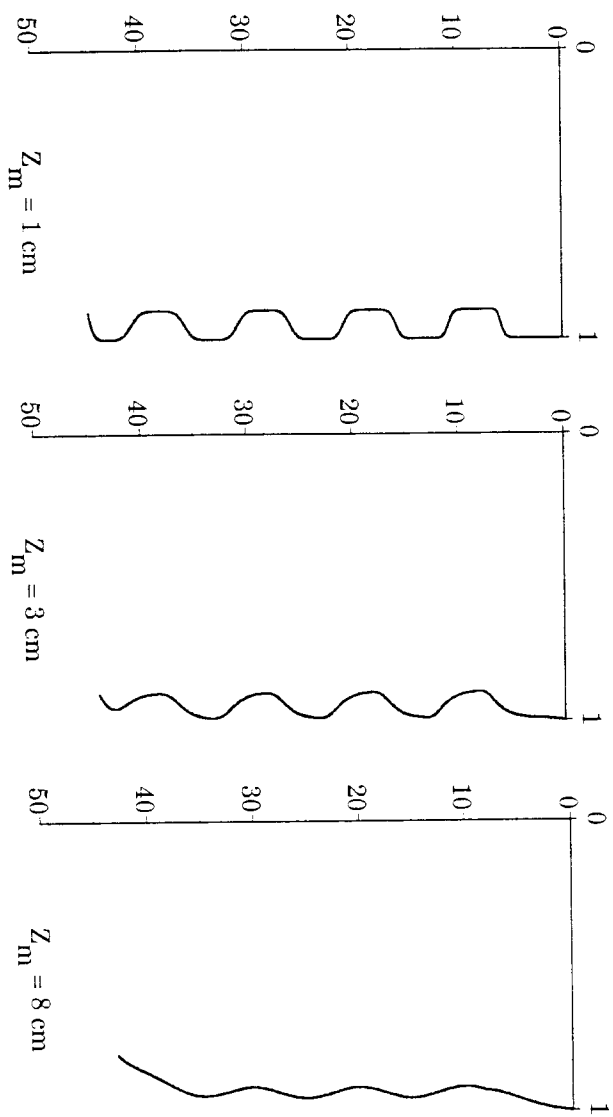




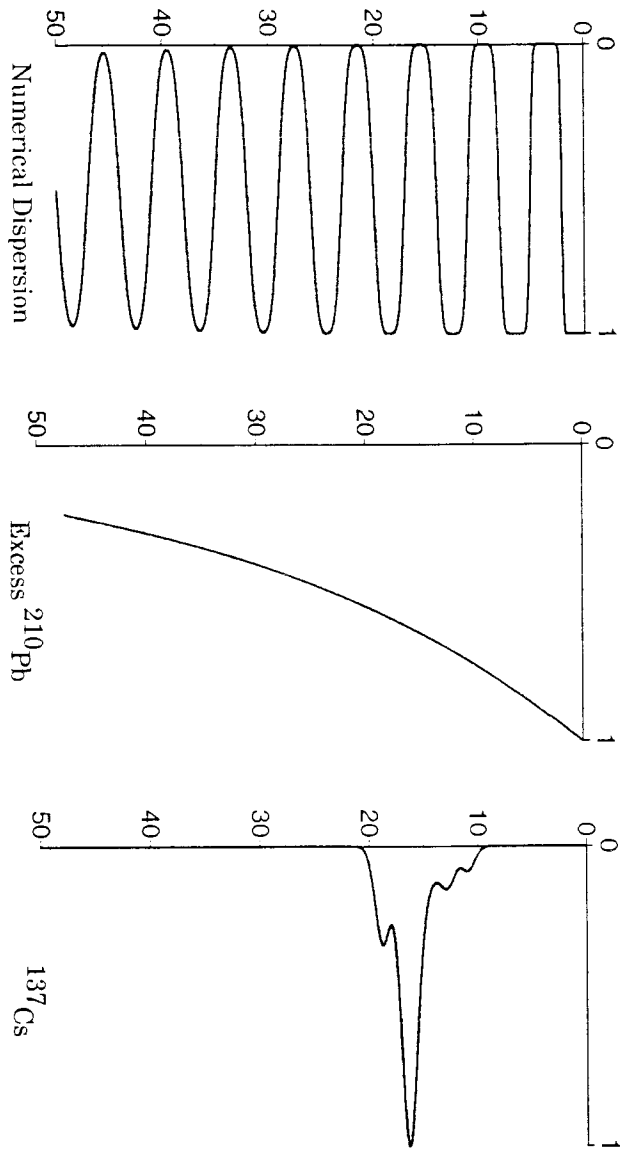
Tracer Concentration (arbitrary units)



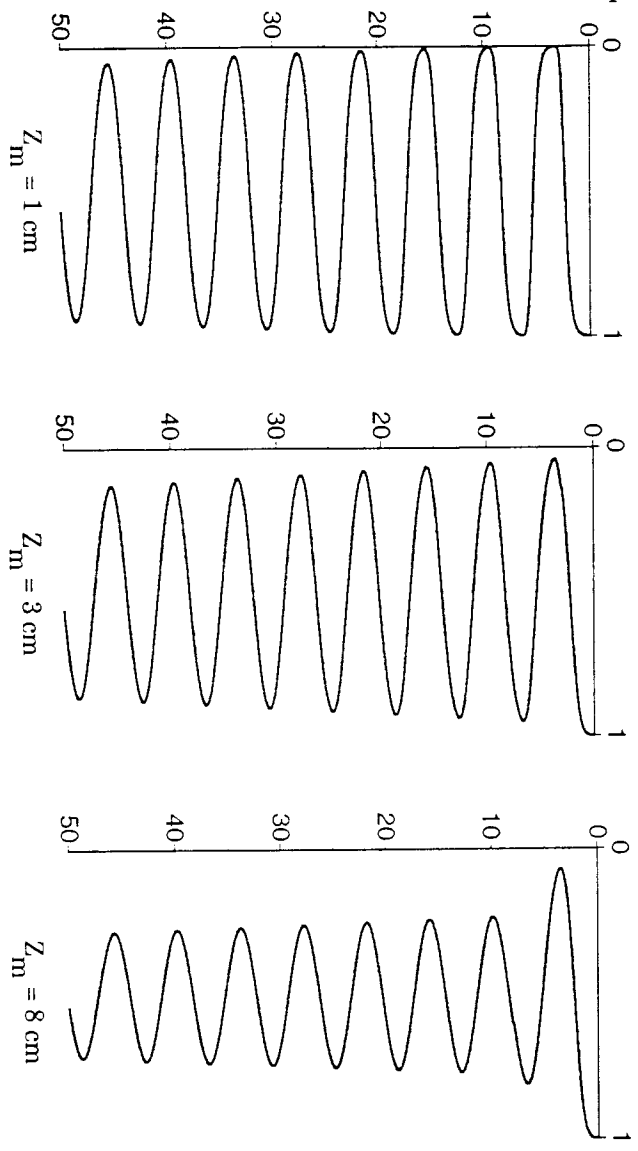
Depth (cm)



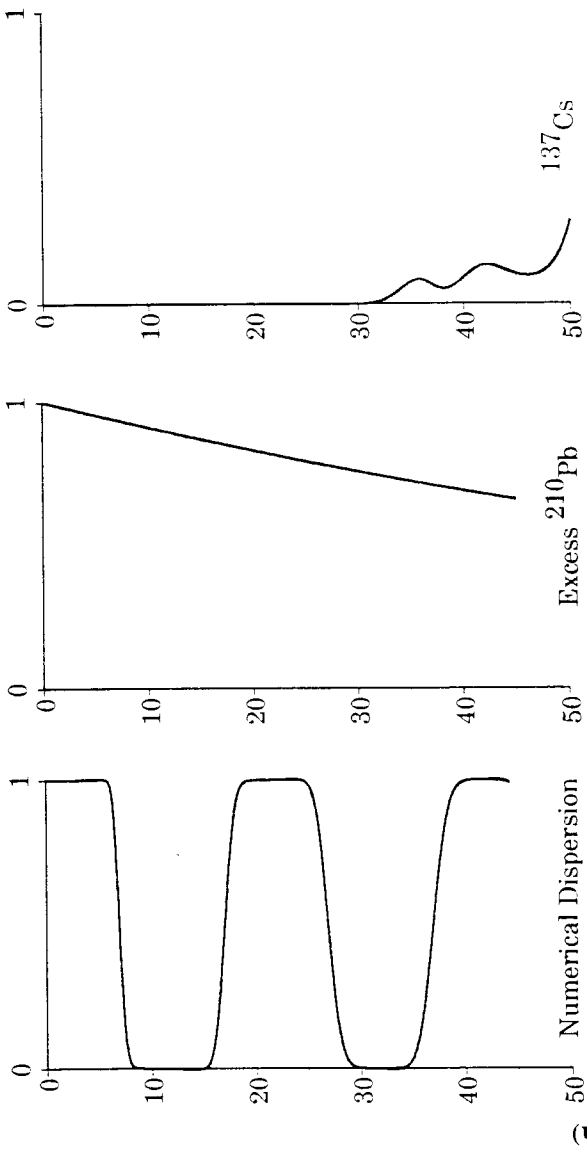
Tracer Concentration (relative units)



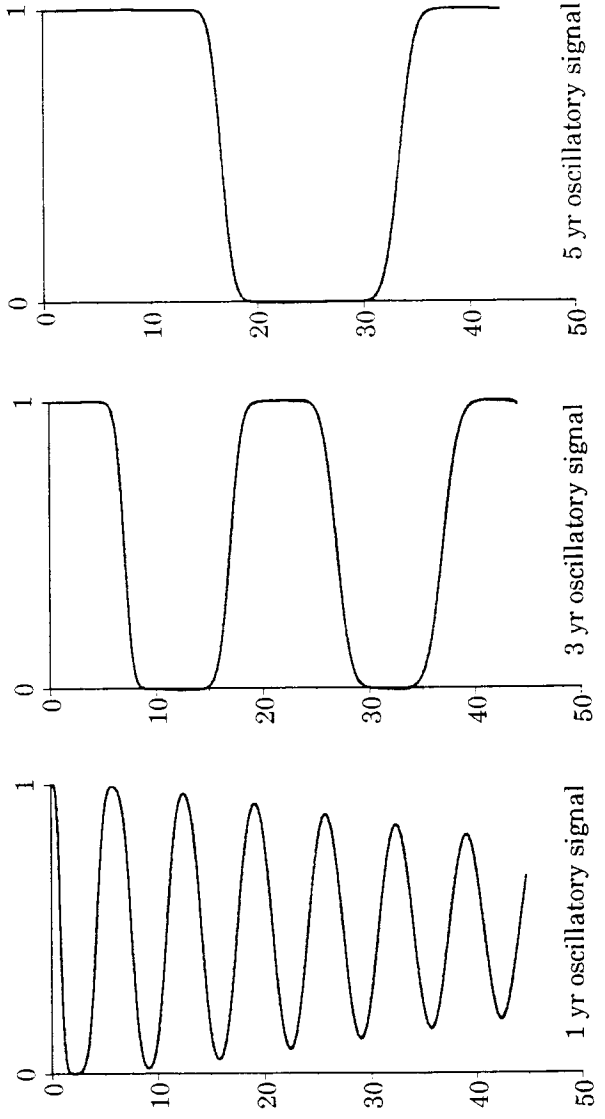
Depth (cm)



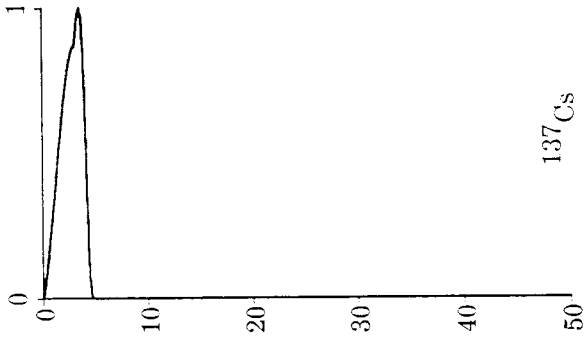
Tracer Concentration (arbitrary units)



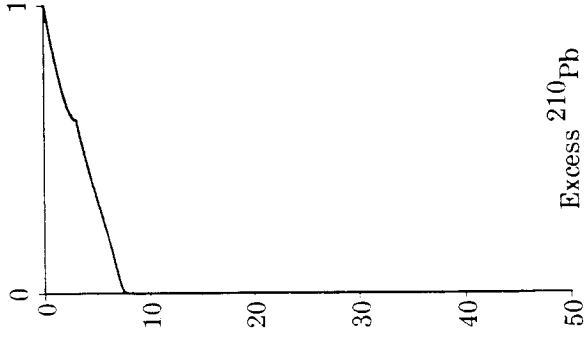
Depth (cm)



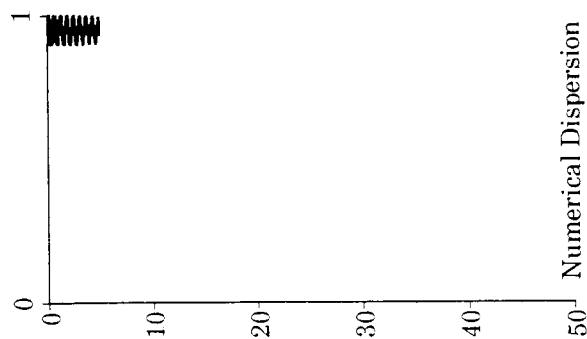
Tracer Concentration (arbitrary units)



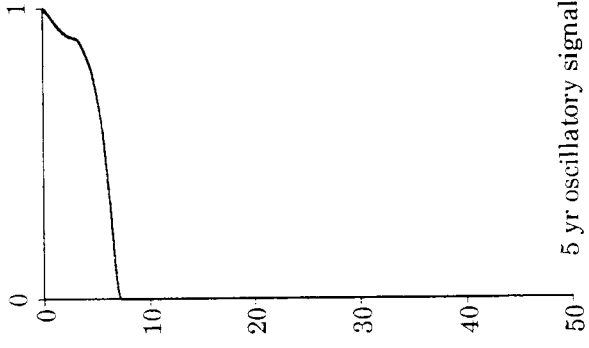
^{137}Cs



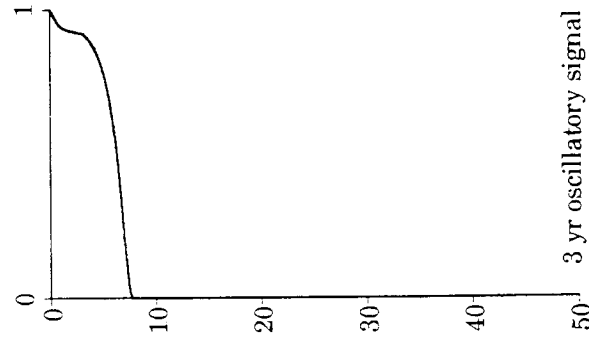
Excess ^{210}Pb



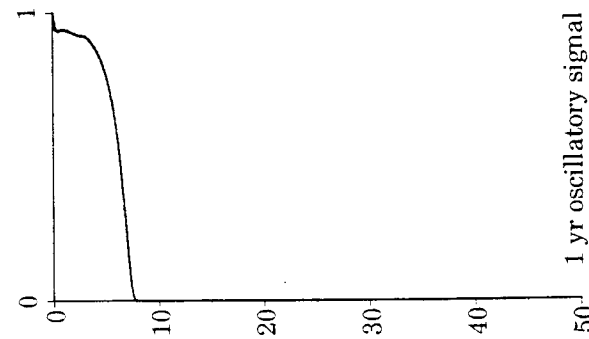
Numerical Dispersion



5 yr oscillatory signal

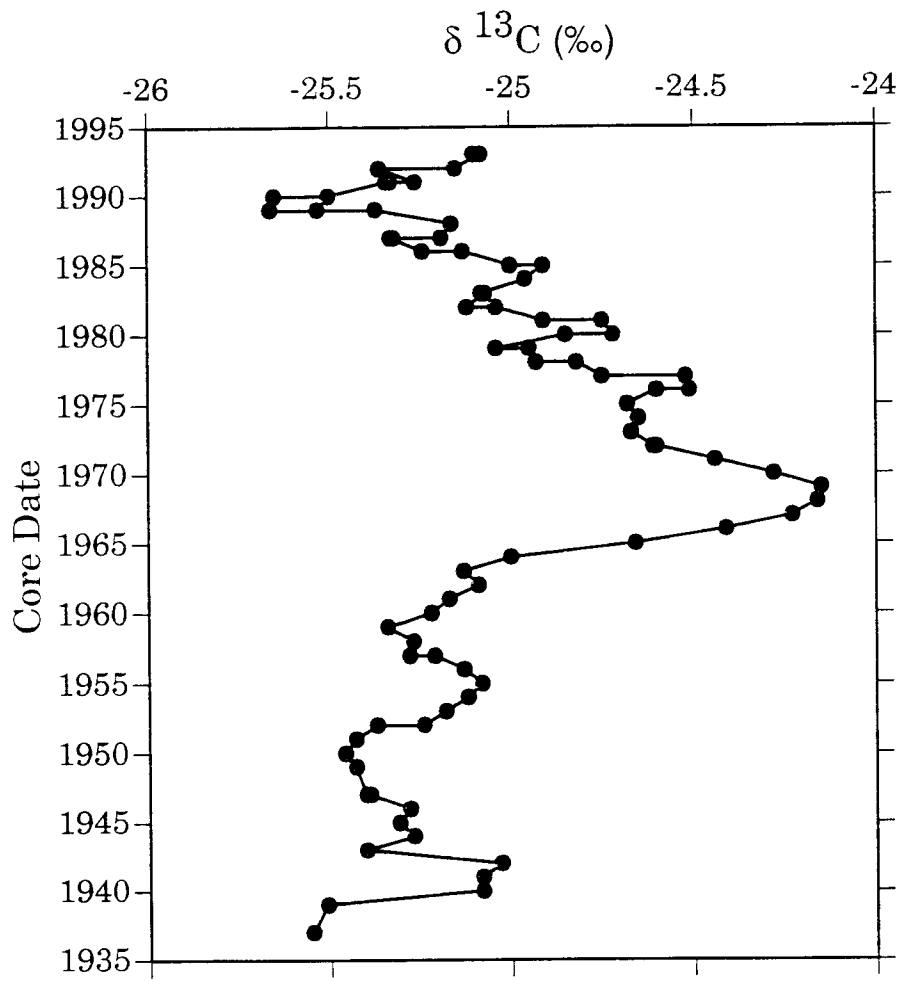


3 yr oscillatory signal



1 yr oscillatory signal

Depth (cm)



Excess ^{210}Pb (relative activity)

